22. Izett, G. A., Maurrasse, F. J-M. R., Lichte, F. E., Meeker, G. P. & Bates, R. *US geol. Survey Open-file Rep.* No. 90-635 (1990).
23. Sigurdsson. H. *et al. Nature* **349**, 482-487 (1991).
24. Erdtmann, G. *Pollen Morphology and Plant Taxonomy* (Chronica Botanica, Waltham, Massachusetts, 1952).

ACKNOWLEDGEMENTS. F. Asaro supplied data on iridium abundance, and B. F. Bohor and G. A. Izett supplied data on distribution of shock-metamorphosed quartz grains. I thank B. F. Bohor, T. M. Bown, A. H. Knoll, D. J. Nichols and R. A. Spicer for critical comments on the manuscript. I thank A. L. Kraps for assistance in the field.

An invasion percolation model of drainage network evolution

Colin P. Stark

Department of Earth Sciences, University of Leeds, Leeds LS2 9JT, UK

STREAM networks evolve by headward growth and branching away from escarpments such as rift margins. The structure of these networks and their topographic relief are known to be fractal[1–3], but no model so far has been able to generate the observed scaling properties. Here I present a statistical model of network growth in which stream heads branch and propagate at a rate that depends only on the local strength of the substrate. This model corresponds to the process of invasion percolation[4], with the added requirement of self-avoidance; it is a self-organized critical system[5] with properties similar to those of standard percolation models[6]. A description based on self-avoiding invasion percolation reproduces the known scaling behaviour of stream networks, and may provide a valuable tool for delineation of drainage patterns from digital topographic data sets[7,8].

Many stochastic models of river network evolution have been proposed, ranging from the early work of Leopold and Langbein[9] on self-avoiding random walks, to the computer simulations of Howard[10] and the aggregation model of Scheidegger[11]. The present study was prompted by the suggestion of Mandelbrot[1] that rivers are fractal. The evidence for this lies in the power-law relation between principal stream length and drainage basin area[12,13]: Hack[14] discovered that the scaling exponent d_H is ≈ 0.6 and not a simple square-root relation as one might expect; such behaviour holds over a remarkable range of scales from laboratory experiments to basins almost the size of the Amazon. The Hack relation may be rewritten:

$$L_p \sim L^{d_{min}} \qquad d_H = d_{min}/2 \qquad (1)$$

where L is drainage basin length, L_p is principal stream length, and d_{min} is the fractal dimension of the principal stream. A reliable estimate[15] for d_H is 0.568.

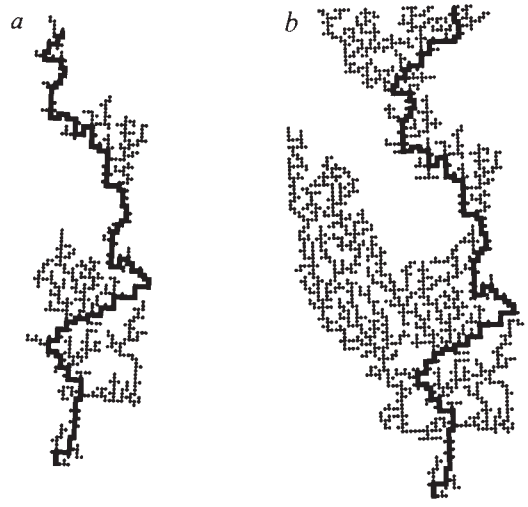

FIG. 1 The development of a self-avoiding invasion percolation cluster, shown at two stages of growth. On average the whole cluster has a fractal dimension of 1.896 and the fractal dimension of the shortest path, marked in heavy type, remains at 1.130 throughout.

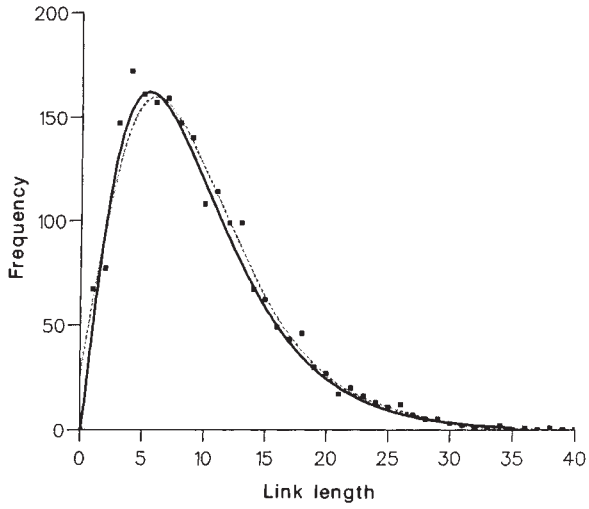

FIG. 2 Distribution of interior-link lengths for the self-avoiding invasion percolation model, from 20 runs on a 256×256 lattice. The bold line is a fit to a gamma function, and the dashed line a smoothed fit to the data points.

In formulating a model of headward growth and branching, we must consider noise in the substrate. Variation in the lithology, structure, diagenesis, groundwater hydrology, soil development, vegetation and topography leads to considerable variation in substrate strength. The manner in which this noise is incorporated into any model of drainage evolution is crucial to the resulting network geometry. Consider a simple model of headward growth of streams away from a rift margin[16] in which stream heads initiate and propagate away from the uplifted escarpment. Bank failure and stream propagation may occur anywhere on the perimeter of the stream network; if the substrate strength varies, however, the probability of failure is far higher at some points on the perimeter than at others. If we make the simplification that at any particular time the next point to fail will be the weakest, the model of headward growth and branching becomes invasion percolation[4]. In invasion percolation, a regular lattice is set up with random strengths assigned to bonds between initially empty sites. The type and dimension of the lattice are not important, nor is the exact distribution of bond strengths. Initially, one seed site is occupied; growth occurs by forming a link along the weakest bond from this seed, and by occupying the linked site. Further growth continues by a similar process around the perimeter of the cluster. The system rapidly self-organizes to a stage where a restricted range of bond strengths is chosen, and the cluster grows indefinitely. The cluster shows the same fractal scaling as standard lattice percolation clusters[6] and as continuum or off-lattice percolation clusters[17].

Streams rarely bifurcate downstream, so a non-looping[18] condition is imposed on growing clusters. This is straightforward to implement: no site may be invaded if any of its neighbour sites except the source site are already occupied. This is a new model which I will call self-avoiding invasion percolation (Fig. 1). Models such as lattice percolation, invasion percolation and self-avoiding invasion percolation all belong to the same universality class[6] and their scaling properties are identical. Hence we can write[19] the distance L_p along a model principal stream as

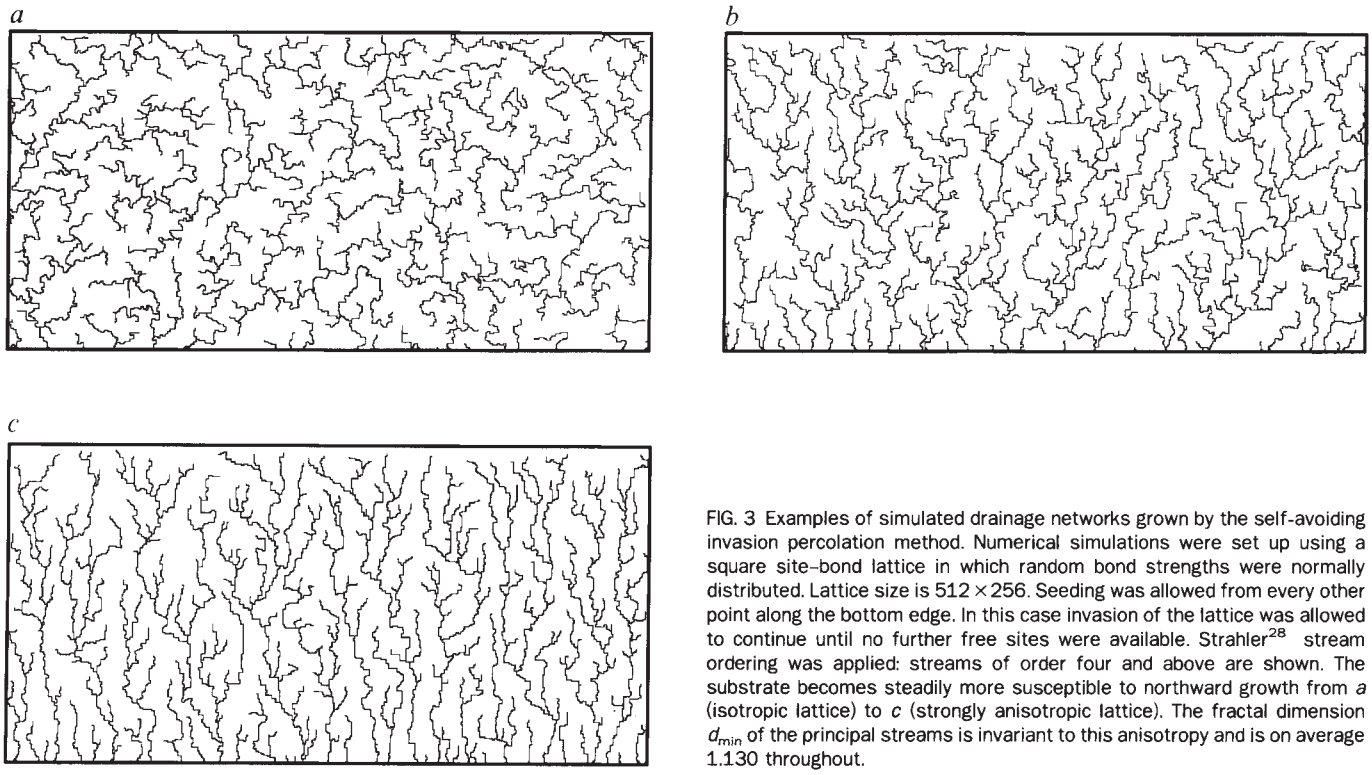

FIG. 3 Examples of simulated drainage networks grown by the self-avoiding invasion percolation method. Numerical simulations were set up using a square site–bond lattice in which random bond strengths were normally distributed. Lattice size is 512 × 256. Seeding was allowed from every other point along the bottom edge. In this case invasion of the lattice was allowed to continue until no further free sites were available. Strahler[28] stream ordering was applied: streams of order four and above are shown. The substrate becomes steadily more susceptible to northward growth from *a* (isotropic lattice) to *c* (strongly anisotropic lattice). The fractal dimension d_{min} of the principal streams is invariant to this anisotropy and is on average 1.130 throughout.

a function of cluster length L as $L_p \sim L^{d_{min}}$ where $d_{min} = 1.130$, the scaling exponent for the cluster backbone[19], and where L is equivalent to drainage basin length. We predict that $d_H = d_{min}/2 = 0.565$. This result is identical to equation (1) and is consistent with the observed[15] value of $d_H \approx 0.568$. It is striking that the model not only predicts fractal scaling of streams but also derives the observed dimension of those streams so accurately. The self-avoiding invasion percolation model predicts other fractal properties for drainage networks; these have been shown recently[20] to be closely related to order ratios for the streams. For example, the stream networks will obey:

$$d_f = \frac{2 \log R_B}{\log R_A} = 1.896 \quad (2)$$

$$d_l = \frac{\log R_B}{\log R_L} = 1.678 \quad (3)$$

where $d_l = d_f/d_{min}$; d_f is the fractal dimension of the whole network, d_l is the intrinsic dimension[17] and R_B, R_L and R_A are the bifurcation, length and area ratios, respectively. Recently obtained values for natural stream networks include $d_f \approx 1.90$, $d_{min} \approx 1.12$ and $d_l \approx 1.65$ from order ratios[13,21], and $d_f \approx 1.90$, $d_{min} \approx 1.16$ from direct (box-counting) fractal measurement[13]. These data are remarkably consistent with the predicted values above. Furthermore, the interior links (the shortest distances between stream junctions) of the model networks are gamma-distributed (Fig. 2), as has been observed for natural systems[22].

An examination of previous models of drainage network evolution shows that few predicted fractal scaling. For example, Howard's computer simulations[10] were essentially Eden tree growth[23]. This is a kinetic model where new sites are added to the perimeter of the cluster at random; in our model this is equivalent to randomly reassigning bond strengths to the lattice at each step. In this system there is no 'history' to the distribution of bond strengths around the growing cluster. The resulting networks are topologically random[24] and Euclidean, with $d_{min} = 1.0$ and $d_f = d_l = 2.0$. The 'top-down' model of Scheidegger[25], in which flow paths coalesce randomly downslope, shows similar scaling. Diffusion-limited aggregation has also been suggested as a suitable model for drainage evolution[16], but fails because the scaling exponent of shortest paths d_{min} on a diffusion-limited aggregate[26] is 1.0. In addition, for such clusters the probability of growth is proportional to the local gradient of the potential field[27]. This potential field ϕ is constrained in the model to obey Laplace's equation, $\nabla^2\phi = 0$, and to be subject to considerable noise. It is not at all clear what potential field determines substrate failure, or whether any such field should satisfy Laplace's equation.

The self-avoiding invasion percolation model can account for substrate sensitivity to local topography without any change in the scaling behaviour of the drainage networks. Similarly, a strong regional tilt may be modelled without affecting the fractal properties of the streams. Figure 3 shows the effect of biasing failure probability in one particular direction: stream networks range from isotropic (*a*) to anisotropic and dendritic (*c*) as the bias is increased, but the fractal scaling of the networks remains invariant. In a percolation model, drainage propagation, controlled by substrate strength, and drainage delineation, controlled by local gradient, are equivalent. This suggests a simple method for drainage delineation in which lattice bond values are calculated by differencing a grid of topographic heights. Streams are then traced out upstream, rather than downstream as is usual, by a self-avoiding growth mechanism. The fractal geometries of stream networks are more likely to be preserved by this method than by existing algorithms.

In conclusion, it seems likely that the dynamical link between surface flow and topography is under-pinned by a self-avoiding invasion percolation process, and that the reason for fractal scaling both of topography[2,3] and drainage networks[1,12,13] may lie in this percolation property of geomorphology. □

Received 19 March; accepted 17 June 1991.

1. Mandelbrot, B. B. *The Fractal Geometry of Nature* (Freeman, New York, 1982).
2. Huang, J. & Turcotte, D. L. *J. geophys. Res.* **94,** 7491–7495 (1989).
3. Thornes, J. *Nature* **345,** 764–765 (1990).
4. Wilkinson, D. & Willemsen, J. F. *J. Phys.* A **16,** 3365–3376 (1983).

5. Bak, P., Tang, C. & Wiesenfeld, K. *Phys. Rev.* A**38,** 364–374 (1988).
6. Stauffer, D. *Introduction to Percolation Theory* (Taylor & Francis, London, 1985).
7. Band, L. E. *Water Resour. Res.* **22,** 15–24 (1986).
8. Jenson, S. K. & Domingue, J. O. *Photogram. Engng Remote Sens.* **54,** 1593–1600 (1988).
9. Leopold, L. B. & Langbein, W. B. *US Geol. Survey Prof. Pap.* 500-A, 1–20 (1962).
10. Howard, A. D. *Geogr. Anal.* **3,** 29–51 (1971).
11. Takayasu, H., Nishikawa, I. & Tasaki, H. *Phys. Rev.* A **37,** 3110–3117 (1988).
12. Hjelmfelt, A. T. Jr *Water Resour. Bull.* **24,** 455–459 (1988).
13. Rosso, R., Bacchi, B. & La Barbera, P. *Water Resour. Res.* **27,** 381–387 (1991).
14. Hack, J. T. *US Geol. Survey Prof. Pap.* 294-B, 1–97 (1957).
15. Gray, D. M. *J. geophys. Res.* **66,** 1215–1223 (1961).
16. Weissel, J. K. *Pacific Rim Congress 90, Proc. v. III,* 63–70 (Austral. Inst. Min. and Metall., Parkville, Vic., 1990).
17. Havlin, S. & Ben-Avraham, D. *Adv. Phys.* **36,** 695–798 (1987).
18. Havlin, S., Nossal, R. & Trus, B. *Phys. Rev.* A **32,** 3829–3831 (1985).
19. Herrmann, H. J. & Stanley, H. E. *J. Phys.* A **21,** L829–L833 (1988).
20. Hinrichsen, E. L., Måløy, K. J., Feder, J. & Jøssang, T. *J. Phys.* A **22,** L271–L277 (1989).
21. La Barbera, P. & Rosso, R. *Water Resour. Res.* **25,** 735–741 (1989).
22. Shreve, R. L. *J. Geol.* **77,** 397–414 (1969).
23. Dhar, D. & Ramaswamy, R. *Phys. Rev. Lett.* **54,** 1346–1349 (1985).
24. Smart, J. S. *Bull. geol. Soc. Am.* **80,** 1757–1774 (1969).
25. Meakin, P. *J. Phys.* A **20,** L1113–L1119 (1987).
26. Meakin, P., Majid, I., Havlin, S. & Stanley, H. E. *J. Phys.* A **17,** L975–L981 (1984).
27. Mandelbrot, B. B. & Evertsz, C. J. G. *Nature* **348,** 143–145 (1990).
28. Strahler, A. N. *Handbook of Applied Hydrology* (ed. Chow, V. T.) 4-II (McGraw-Hill, New York, 1964).

ACKNOWLEDGEMENTS. I thank M. J. Kirkby, M. R. Leeder and J. A. Stark for discussions, and the NERC for financial support.

Sources of sedimentary lipids deduced from stable carbon-isotope analyses of individual compounds

Gareth Rieley*, Robert J. Collier*, David M. Jones*, Geoffrey Eglinton*, Paul A. Eakin† & Anthony E. Fallick†

* Organic Geochemistry Unit, School of Chemistry, University of Bristol, Cantock's Close, Bristol BS8 1TS, UK
† Scottish Universities Research and Reactor Centre, East Kilbride, Glasgow G75 0QU, UK

COMPOUND-specific isotope analysis by gas chromatography combined with isotope-ratio mass spectrometry (GC–IRMS)[1,2] provides a new tool with which to study the carbon cycle at the molecular scale[3]. Previous studies[2,4] using this technique have been concerned with oceanic systems. Here we demonstrate that the potential for elucidating terrestrial sedimentary processes is equally important. By comparing the carbon isotope ratios ($\delta^{13}C$) of individual *n*-alkanes from the leaves of lakeside trees with those from the lake sediments, we are able to discriminate between the diverse sources of the sedimentary carbon. The leaf-wax *n*-alkanes show a large inter-species $\delta^{13}C$ variation of −30.1 to −38.7‰, which may be the result of genetic differences in plant adaptation and physiology. Values of −30.1 to −35.9‰ were obtained for the corresponding *n*-alkanes extracted from the lake sediments, indicating that they derive from a mixed input of deciduous leaf waxes. Shorter-chain lipids in the sediments had $\delta^{13}C$ values of −20 to −22‰, implying that these originate from a different (probably algal) source. Information of this sort goes beyond that which can be deduced from bulk isotope or biomarker analyses alone.

Measurement of carbon isotope ratios in bulk organic matter has become widely used. For example, carbon isotope discrimination in relation to plant physiology has been extensively investigated[5–10] and variations in $\delta^{13}C$ values in terrestrial C3 plant tissue have been attributed to factors that affect the internal concentration of carbon dioxide in the leaf[8], such as light irradiation[9], efficiency of water use[7] and stomatal resistance[10].

Comparison of $\delta^{13}C$ data for bulk plant biomass with values for organic carbon from sedimentary cores has assisted in the reconstruction of ancient biogeochemical processes[11]. GC–IRMS[1] now permits this comparison to be carried out at the molecular level, resulting in a much more detailed picture of the biogeochemistry of sedimentary ecosystems[2,4]. Earlier studies have dealt with ancient aquatic systems, in which the fractionation of carbon isotopes is related to the concentration of dissolved bicarbonate in water[4]. In terrestrial plants, however, $\delta^{13}C$ is related to CO_2 gas-exchange factors operating in air[6,7]. The $\delta^{13}C$ information currently available for individual compounds in terrestrial plants or fresh-water sedimentary organic matter is very limited and based on lengthy separation techniques, with $\delta^{13}C$ analyses by conventional combustion IRMS[12,13]. With GC–IRMS, such analyses can be carried out simply and routinely[2,4], allowing stable isotope research to be applied in many diverse disciplines[3].

We sampled six deciduous tree species growing close to each other around Ellesmere lake[14] (United Kingdom) in November 1989. Three samples of sediment from a short core taken from the lake were examined for comparison. The sampling, extraction methods and detailed lipid distributions are described by Rieley *et al.*[15]. The $\delta^{13}C$ measurements reported here for the *n*-alkane fractions were obtained using a VG Isochrom II GC–IRMS; a representative ion-current chromatogram at relative molecular mass $M_r = 44$ is given in Fig. 1.

The $\delta^{13}C$ results for the individual *n*-alkanes and *n*-alcohols are given in Table 1. Values of $\delta^{13}C$ for the *n*-alkanes C_{25} to C_{33} in the sediment samples vary from −30.1 to −35.9‰, which are consistent with bulk values for higher plants following the C3 metabolic pathway[16]. These values are much more negative than those of other aliphatic lipids assigned to an autochthonous (algal) source in the same sedimentary system, which had $\delta^{13}C$ = −22.7 and −23.8‰ for the C_{14} and C_{16} *n*-alcohols[17], respectively. Furthermore, the mean $\delta^{13}C$ values for the leaf-wax *n*-alkanes in the same carbon-number range vary from −30.1 to −38.4‰. Thus, the sedimentary *n*-alkanes and *n*-alkanols in the range C_{25} to C_{33} can be attributed primarily to the input of leaves from deciduous trees fringing the lake. The advantage of GC–IRMS over conventional isotope analyses of bulk organic carbon is illustrated by this discrimination between compounds originating from fresh-water algae and from terrestrial plants. In contrast, the two sediment samples taken from 0–5 cm and 10–15 cm in Ellesmere had $\delta^{13}C$ values for total organic carbon that were identical (−27.4‰), representing an averaging of all possible sources and of the products of diagenesis. The identical bulk $\delta^{13}C$ values could be interpreted as indicating a constant source for the sedimentary carbon, whereas the GC–IRMS

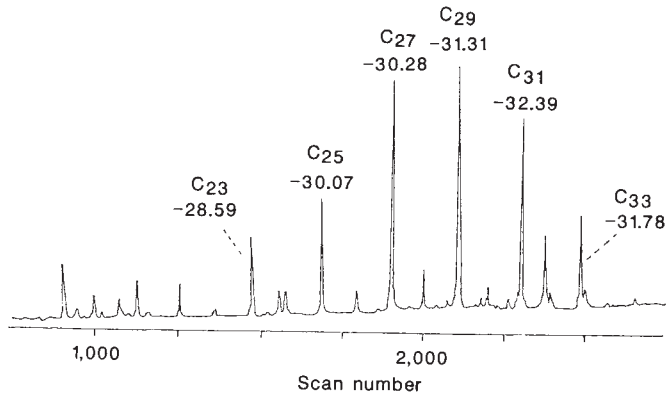

FIG. 1 Hydrocarbon fraction from Ellesmere sediment at 10 to 40 cm depth. This is the relative molecular mass $M_r = 44$ ion-current chromatogram, obtained from the continuous analysis of the combusted GC effluent by a mass spectrometer[1]. The *n*-alkane carbon numbers are given above $\delta^{13}C$ values for each peak analysed. GC column: 25 m × 0.32 mm internal diameter fused silicone (CP SIL 5CB); helium carrier gas; temperature programme, increasing from 80–300° at a rate of ~4° min^{-1}, then isothermal at 300° for 20 min. $\delta^{13}C = [(R_{sample}/R_{standard}) - 1] \times 10^3$‰ PDB, where $R = {}^{13}C/{}^{12}C$ and $R_{standard} = 0.0112372$ based on Pee Dee belemnite.